CEST 2021

17th International Conference on Environmental Science and Technology

Athens, Greece, 1 to 4 September 2021

CO abatement via Ir-based catalysts: effect of the support and preparation method on catalytic activity and stability

DROSOU C.[1], **FOUNTOULI T.V.**[1], **STRATAKIS A.**[2], **CHARISIOU N.D.**[3] **GOULA M.A.**[3,*] **and YENTEKAKIS I.V.**[1,*]

[1] Laboratory of Physical Chemistry & Chemical Processes, School of Chemical & Environmental Engineering, Technical University of Crete, GR-73100 Chania, Greece

[2] School of Mineral Resources Engineering, Technical University of Crete, GR-73100 Chania, Greece

[3] Department of Chemical Engineering, University of Western Macedonia, GR-50100, Greece

*corresponding authors:
e-mail: yyentek@isc.tuc.gr (I.V. Yentekakis); mgoula@uowm.gr (M.A. Goula)

Abstract. Here we report on the effect of the support and preparation method on the activity and stability of Ir-based catalysts under CO oxidation. Alunina-ceria-zirconia (ACZ: 60wt%Al_2O_3 - 40wt%$Ce_xZr_{1-x}O_2$, x=0.25, 0.5, 0.75) mixed oxide supports with high oxygen storage capacity (OSC) were synthesized via two different methods, hydrothermal (ACZ-H) and co-precipitation (ACZ-P), and used as supports of Ir nanoparticles, so as, besides the Ce/Zr composition to also deal with the effect of the preparation method on catalytic performance. ACZ supports and counterpart Ir/ACZ catalysts were thoroughly characterized using various techniques, while catalytic measurements were conducted under excess O_2 conditions (1.0% CO, 5.0% O_2, balance He at 1 bar) in the temperature range of 100-400°C. Both pre-reduced and pre-oxidized catalysts were evaluated, while their sintering behavior after experiencing several sequential oxidative thermal aging steps was also studied. The results demonstrated superior textural characteristics (BET surface area and pore volume) of Ir/ACZ-H catalysts as well as stronger interaction of Ir nanoparticles and support particles than that of Ir/ACZ-P, resulting to better CO oxidation efficiency and stability. All catalysts demonstrated stable CO activity after thermal aging, reflecting beneficial influence of ACZ support on the sintering resistance characteristics of Ir nanoparticles.

Keywords: CO oxidation, Iridium, Alumina-ceria-zirconia

1. Introduction

CO is a toxic gas that affects the quality of human health and is included among the major air pollutants (Kim et al., 2020). The main sources of CO emissions are automobiles, power plants, and the petrochemical industry (Chen et al., 2006). Catalytic CO oxidation is an extremely widespread reaction to convert CO to CO_2 for reducing air pollution. In addition, CO oxidation is an important reaction in the process of H_2 production via hydrocarbons reforming, since the selective removal of CO from reformate (CO+H_2) by means of the so-called *preferential oxidation* (PROX) of CO is an attractive, efficient and cost-effective process (Liu et al., 2012).

A suitable catalyst for CO oxidation must present high activity at low temperatures and remain stable at high temperatures. The reaction has been for many years one of the most extensively studied catalytic reactions. Interest continues to be high (Zhang et al. 2020), and in recent years CO oxidation has been extensively investigated in various alternative catalytic systems, including: (i) noble metals, such as Au (Liu et al., 2017), Pt (Yentekakis et al., 1988), Pd (Wang et al., 2017), (ii) non-noble metals, such as Cu (Zou et al., 2018), Ni (Wang et al., 2019) and (iii) metal-free materials (Esrafili et al., 2019). Among these catalytic systems, noble metals provide high activity even at low temperatures, and for this reason, despite their limited availability and high cost, they are widely used (Kim et al., 2020). Although, Ir is significantly cheaper than other noble metals also offering high efficiency on the abatement of CO and various air pollutants (NO_x, N_2O and hydrocarbons) that typically coexist with CO in effluent gases, its use on pollutants' abatement processes still remains limited as a result of its high propensity to agglomerate at elevated temperatures and oxidative environments (Yentekakis et al., 2018). However, it was recently demonstrated that metal nanoparticles dispersed on supports with high oxygen ion lability and oxygen storage capacity (OSC), such as ceria- and/or zirconia-containing mixed oxides, are endowed with remarkable resistance to thermal sintering under oxidative conditions (Yentekakis et al., 2016 and 2018; Goula et al., 2019). On the other hand, CeO_2 is widely used as a typical stabilizer and promoter of the Al_2O_3 washcoat in last generation three-way automotive catalysts due to its excellent properties including increased thermal stability of Al_2O_3, enhanced dispersion of the metal on the support and especially high oxygen storage/release capacity (OSC), while ZrO_2 insertion in CeO_2 further improves the aforementioned desirable properties (Di Monte et al., 2004; Papavasiliou et al., 2009; Li et al., 2020).

In the present study the effect of the support nature and preparation method on the CO abatment catalytic activity and stability of nanostructured 1.0 wt% Ir-based catalysts is investigated in detail. More specifically, the effect of 60wt% Al_2O_3 - 40wt% $Ce_xZr_{1-x}O_{2-\delta}$ (ACZ) mixed oxide support with varying Ce/Zr composition (x=0.25, 0.5 and 0.75) on both activity and stability of Ir nanoparticles supported on it, is investigated at the temperature range 100-400°C and excess O_2 conditions typically used in lean-burn, diesel and fossil fuel stationary combustion processes. The ACZ mixed oxide support was prepared following (i) a co-precipitation and (ii) a hydrothermal method in order this study to deal with the effect of the preparation method on catalysts' performance, as well. Substantial influences of both support composition and preparation method on the CO oxidation catalytic performance were recorded.

2. Experimental

2.1. Catalysts preparation

2.1.1 Supports preparation:

ACZ mixed oxide supports were synthesized by a co-precipitation method and a hydrothermal method hereafter denoted as ACZ-P and ACZ-H, respectively. Similar precursor salts, namely $Al(NO_3)_3{\cdot}9H_2O$ (98%, Fluka), $Ce(NO_3)_3{\cdot}6H_2O$ (99%, Sigma-Aldrich) and $ZrO(NO_3)_2{\cdot}xH_2O$ (99%, Sigma Aldrich),were used in both cases with the approprtiate weight in order to obtain the desired composition of 60 wt% Al_2O_3 and 40wt% CeO_2-ZrO_2 with Ce/Zr molar ratios of 0.25/0.75, 0.5/0.5 and 0.75/0.25 in the final mixed oxide product. More specifically: The ACZ-P supports were prepared by the co-precipitation method described in detail alsewere (Papavasileiou et al., 2009). In brief, specified amounts of the 0.5 M aqueous solutions made by the aforementioned aluminium, cerium and zircinium nitrate salts were mixed and a precipitating agent (NH_3, 25 v/v%) was added at room temperature until the pH was stabilized at ~9 under continuous stirring for 3h. The resulting precipitate was filtered, dried at 110 °C, and calcined at 800 °C for 2 h in air. The ACZ-H supports were prepared via a facile hydrothermal method, according to Li et al., 2020. Predetermined amounts of Al, Ce and Zr nitrate precursors were first dissolved in a specified amount of de-ionized water. Afterward, the mixed solution was precipitated using a buffer solution of $NH_3{\cdot}H_2O$ (3 mol/L) and $(NH_3)_2CO_3$ (3 mol/L) under continuous stirring at a pH value of 9. The precipitated mixed salt hydroxide, along with its supernatant liquid, was then transferred in a Teflon-lined stainless steel autoclave and hydrothermally treated at 100°C for 20 h. The precipitate was then obtained via centrifugation and further washed 2 times with de-ionized water. Then it was dried at 110°C overnight and calcined at 800°C for 2 h in air.

2.1.2 Ir catalysts preparation

Iridium was introduced on the ACZ-P and ACZ-H supports via the wet impregnation as follows. In a aqueous solution of 2 mg Ir/mL, obtained by disolving $IrCl_3{\cdot}xH_2O$ (99.9%, Abcr) in de-ionized water, the appropriate amount of the ACZ support was impregtated so as to achieve an Ir loading of 1 wt% in the final catalyst. The resulted slurry was slowly evaporated at 75°C for 5h using a rotary evaporator and then dried at 110° C, overnight. The dried sample was then directly reduced at 400 °C for 3 h under 25 % H_2 flow (balanced with He) for the effective removal of residual chlorine originated for the decomposition of the cloride precursor, but also to avoid formation of large IrO_x aggregates, as demonstrated elsewere (Yentekakis et al., 2016). Using the above methods six catalysts were prepared as listed in Table 1.

Table 1. Textural and morphological characteristics of supports and catalysts studied.

Catalyst	Ce/Zr	S_{BET} (m^2/g_{cat})		Ir dispersion (%)
		Support	Catalyst	
Ir/ACZ-H1[a]	0.25/0.75	154	216	66
Ir/ACZ-H2[a]	0.5/0.5	172	184	66
Ir-ACZ-H3[a]	0.75/0.25	149	157	70
Ir-ACZ-P1[b]	0.25/0.75	113	134	70
Ir-ACZ-P2[b]	0.5/0.5	102	100	81
Ir-ACZ-P3[b]	0.75/0.25	115	125	70

Catalyst supports synthesized by hydrothermal (a) *or co-precipitation* (b) *method.*
(c)*: calculated from XRD data via Scherrer equation.*

2.2. Materials characterization

The textural characteristics of prepared ACZ supports and counterpart Ir/ACZ catalysts were determined by the N_2 physical adsorption-desorption isotherms obtained at -196 °C, using a Nova 2200e Quantochrome instrument. BET surface areas (S_{BET}) were obtained according to Brunauer-Emmett-Teller (BET) method, total pore volume was calculated based on nitrogen volume at the highest relative pressure and the average pore size diameter was determined by the Barrett-Joyner-Halenda (BJH) model.

X-ray powder diffraction (XRD) analysis was performed on a BrukerAXS D8 Advance diffractometer at 35 kV and 35 mA with Cu Kα radiation and LynxEye detector with Ni-filter. The measurements were carried out in the 2θ angle range of 4–70 degrees with a scanning speed of 0.5 degrees per minute. The average particle size of different phases was calculated with the Scherrer equation, based on their most intense diffraction peaks. The quantification of the phases in the samples was performed with the Rietveld method using BrukerAXS Topas software (COD, Crystallography Open Database).

Hydrogen temperature programmed reduction (H_2-TPR) measurements were performed by a Quantachrome/ ChemBet Pulsar TPR/TPD chemisorption analyzer equiped with an Omnistar/Pfeiffer Vacuum mass spectrometer. The total amounts of consumed hydrogen were used to calculate the total oxygen storage capacity (OSC) values of the ACZ supports and counterpart Ir/ACZ catalysts.

Mean Ir particle sizes and thus Ir dispersion was determined by isothermal hydrogen chemisorption (H_2-Chem) measurements acquired on the same apparatus used in H_2-TPR experiments. Samples preparation before aquisition of the H_2-TPR and H_2-chem. mesurements can be found elsewhere (Goula et al., 2019).

2.3. Catalytic activity and thermal stability

Catalytic activity and thermal stability of the catalysts were studied using a 3 mm internal diameter tubular quartz, fixed-bed reactor, loaded with 30 mg of catalyst. A feed composition of 1% CO, 5% O_2 balanced with He at 1 bar was used with a total flow rate of 160 cm^3/min, i.e. a weight-basis gas hourly space velocity (wGHSV) equat to 320,000 mL·g_{cat}^{-1}·h^{-1}. The excess oxygen reaction conditions was chosen to mimit several practical emissions control catalytic processes, e.g. lean-burn and diesel exhaust gases, or stationary fossil fuel combustion effluents. Catalytic activity measurements were obtained on both pre-reduced and pre-oxidized catalysts. Pre-reduction was performed with a 25% H_2/He flow (50 cm^3/min) at 350ºC for 0.5 h, and pre-oxidation with a 20% O_2/He flow (50 cm^3/min) at 400ºC for 1h. Reactants and products analysis was performed using on line GC chromatography (Shimadzu 14 B, TC detector, He carrier gas). Catalyst activity as a function of temperature (*light-off* profiles) was conducted in the temperature range of 100-400ºC. In order to study the voulnerability of Ir nanoparticles dispersed on ACZ suppotrs, sequencial oxidative sintering experiments were perforrmed with all six samples during which the samples were subjected to the following aging protocol: two consecutive oxidation steps at 600°C followed by two additional at 700°C, each oxidation step lasted 2 hours at a flow rate of 20 v/v% O_2/He (40 mL/min); between these oxidation steps, the catalysts were rapidly reduced (0.5 h at a flow of 25 v/v% H_2/He, 100 mL/min at the same temperature) before being subjected to the same reaction conditions (1% CO, 5% O_2, balance He; T=320ºC) for evaluating its catalytic activity.

3. Results and discussion

3.1. Materials characterization results

In Table 1 the textural and morphological characterists of ACZ supports and counterpart Ir/AZC catalysts are summarized. According to the results, both ACZ supports and Ir/ACZ catalysts prepared by the hydrothermal method show relatively larger surface areas compared to the corresponding supports and catalysts prepared by the co-precipitation method. Insignificant surface area changes resulted by increasing Ce content from 0.25 to 0.75% in CZ component of the catalysts; Zhu et al., 2013 found progressive improvements in surface area values by increasing the content of Ce. The addition of iridium causes an increase of the surface area in both groups of ACZ materials probably due to its high dispersion and/or the partial reconstruction of the supports during the impregnation step.

H_2-chemisoprtion results showed that Ir dispersion was high enough, in the order of ca. 66-81% (Table 1), and slightly better on ACZ supports prepared by co-precipitation (Table 1). Coresponding Ir crystallite sizes were varied in the range of 0.9-1.1 nm.

H_2-TPR results revealed catalyst OSC values in the range of ca. 190-210 μmol O_2/g_{cat}. Regarding this property, the catalysts prepared by the hydrothermal method were slightly superior. It is also worth noting that the TPR peaks corresponding to Ir particles were wider and shifted to slightly higher temperatures in the hydrothermally prepared catalysts, compared to those prepared by co-precipitation, suggesting a stronger interaction between iridium and support.

XRD results revealed that a ceria-zirconia solid solution with cubic fluorite phase and the main crystal structure of $Ce_{0.5}Zr_{0.5}O_2$ is formed in all ACZ-containing samples with crystallite sizes of ca. 8.5-12.6 nm, while CeO_2 and ZrO_2 oxides at a significantly lower content were also found. According to the literature, as the ZrO_2 content is increased, there is a slight shift of the peaks at a greater angle 2θ (Kim et al., 2009). This is also observed in our XRD results; the theoretical value of the $Ce_{0.5}Zr_{0.5}O_2$ mixed oxide is $2\theta = 28.9^o$, and a shift of the peak between 28.5° (CeO_2) $<2\theta<30.3^o$ (ZrO_2) depending on the Zr-content of the sample was found. In addition, comparing the two preparation methods, hydrothermal and co-precipitation, the peaks of the samples prepared by the former method were sharper suggesting better crystallites formation (Zhang et al., 2009). Peaks corresponding to Ir phases are not detectable due to the small size of the Ir particles, in agreement to H_2 chemisorption results.

3.2. Activity and thermal stability results

Fig. 1 shows the *light-off* profiles of the pre-reduced (Fig. 1a) and pre-oxidized (Fig. 1b) catalysts at constant reactor feed composition. Pre-reduced catalysts were more active than pre-oxidized ones, ignited respectively at ca. 125ºC and 175ºC. That is, metallic Ir^0 is more active than IrO_2 in CO oxidation. It is also apparent that hydrothermally synthesized catalysts are more active compared to their counterpart catalysts made via co-precipitation, since their *light-off* profiles are shifted up to ~40ºC lower temperatures in the case of pre-reduced and up to ~10ºC in the case of pre-oxidized catalysts (Figs. 1a and b; Table 2). The hydrothermally synthesized Ir/ACZ-H1 catalyst with a Ce/Zr = 0.25/0.75 is the best from all six catalysts studied.

Table 2. Temperatures for 50% CO conversion (T_{50}).

Catalyst	**T_{50} (ºC)**	
	Pre-reduced	Pre-oxidized
Ir/ACZ-H1[a]	207	287
Ir/ACZ-H2[a]	245	290
Ir-ACZ-H3[a]	236	300
Ir-ACZ-P1[b]	245	290
Ir-ACZ-P2[b]	264	301
Ir-ACZ-P3[b]	255	309

Moreover, activity tests on the catalysts after imposition of sequential steps in oxidative thermal aging conditions (specifically: 1st step: 600ºC for 2h; 2nd step: 600ºC 2h; 3rd step: 700ºC 2h; 4th step: 700ºC 2h – all steps in 50 mL/min of 20%O_2/He flow), revealed that all catalysts were particularly stable in terms of their CO oxidation activity measured between these steps. It is well known that in such conditions Ir particles have a high propensity to agglomerate. However, anti-sintering mechanisms – such as recently described by Yentekakis et al., 2016 and Goula et al., 2019 – which are motivated by supports with high OSCs (as the ACZ support used herein) endow Ir particles with excellent sinter-resistance properties. Hydrothermally synthesized catalysts were found to be extremely stable, while co-precipitated catalysts were slightly inferior in stability.

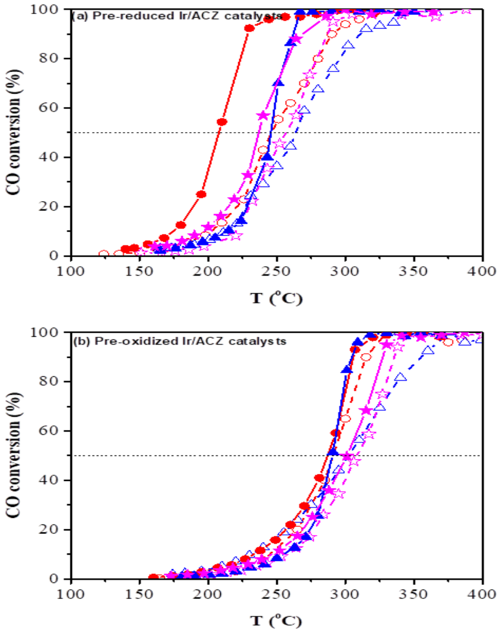

Figure 1. CO conversion light-off profiles on pre-reduced (a) and pre-oxidized (b) Ir/ACZ catalysts. Experimental conditions: 1 v/v% CO, 5 v/v% O_2 balanced with He; wGHSV=320,000 mL·g_{cat}^{-1}·h^{-1}. Filled symbols, solid lines: hydrothermally synthesized catalysts; open symbols, dashed lines: catalysts synthesized by co-precipitation. Circles: Ir/ACZ-H1 and Ir/ACZ-P1 (Ce/Zr=0.25/0.75); triangles: Ir/ACZ-H2 and Ir/ACZ-P2 (Ce/Zr=0.25/0.5); stars: Ir/ACZ-H3 and Ir/ACZ-P3 (Ce/Zr=0.25/0.75).

4. Conclusions

Ir/ACZ catalysts prepared by a hydrothermal method are more active in CO oxidation reaction compared to counterpart catalysts prepared by co-precipitation. The higher interaction of Ir particles with the support is most likely the origin of this superiority. Pre-reduced catalysts are significantly more active than pre-oxidized ones, indicating that metallic Ir instead of IrO_2 is the optimal active phase in CO oxidation reaction. In terms of catalyst composition, the Ir/ACZ-H1 catalyst with a Ce/Zr ratio of 0.25/0.75 was the best in CO oxidation efficiency.

Acknowledgements

Financial support by the GREEK-CHINESE BILATERAL RESEARCH AND INNOVATION COOPERATION, 2018-2021 program (Project No: T7ΔΚΙ-00356) is gratefully acknowledged.

References

Chen W., et al., (2006), Structure sensitivity in the oxidation of CO on Ir surfaces, *Langmuir*, **22**, 3166-3173.

Di Monte R., […] and Fonda E. (2004), Thermal stabilization of $Ce_xZr_{1-x}O_2$ oxygen storage promoters by addition of Al_2O_3: Effect of thermal aging on textural, structural, and morphological properties, *Chem. Mat.*, **16** (22) 4273-4285.

Esrafili M.D, and Heydari S. (2019), A promising and new single-atom catalyst for CO oxidation: Si-embedded MoS_2 monolayer, J. Phys. Chem. Solids, **135**, 109123.

Goula G., Botzolaki G., […]and Yentekakis I.V. (2019), Oxidative thermal sintering and redispersion of Rh nanoparticles on supports with high oxygen ion lability, *Catalysts*, **9**, 541.

Kim H.J., et al., (2020), Design of ceria catalysts for low-temperature CO Oxidation, *ChemCatChem*, **12**, 11-26.

Kim J.-R., et al., (2009), Characteristics of CeO_2–ZrO_2 mixed oxide prepared by continuous hydrothermal synthesis in supercritical water as support of Rh catalyst for catalytic reduction of NO by CO, *J. Catal.*, **263**, 123-133.

Li S., Deng J., Dan Y., Xiong L., Wang J. and Chen Y. (2020), Designed synthesis of highly active CeO_2-ZrO_2-Al_2O_3 support materials with optimized surface property for Pd-only three-way catalysts. *Appl. Surf. Sci.*, **506**, 144866.

Liu K., Wang A. and Zhang T. (2012), Recent advances in preferential oxidation of CO reaction over platinum group metal catalysts, *ACS Catal.*, **2**, 1165–1178.

Liu J.C., Wang Y.G. and Li J. (2017), Toward rational design of oxide-supported single-atom catalysts: Atomic dispersion of gold on ceria, *J. Am. Chem. Soc.*, **139**, 6190–6199.

Papavasiliou A., […] Yentekakis I.V. and Boukos N. (2009), Development of a Ce–Zr–La modified Pt/γ-Al_2O_3 TWCs' washcoat: Effect of synthesis procedure on catalytic behavior and thermal durability, *Appl. Catal. B*, **90** 162-174.

Wang X., Chen J., Zeng J., […] and Zheng L. (2017), The synergy between atomically dispersed Pd and cerium oxide for enhanced catalytic properties, *Nanoscale*, **9**, 6643-6648.

Wang H., […] and Yang M. (2019), Single-site Pt/La-Al_2O_3 stabilized by Ba as an active and stable catalyst in purifying CO and C_3H_6 emissions, *Appl. Catal. B*, **244**, 327-339.

Wang L.-N., Li X.-N. and He S.-G. (2019). Catalytic CO oxidation by noble-metal-free $Ni_2VO_{4,5}$–clusters: A CO self-promoted mechanism, *Phys. Chem. Lett.*, **10**, 1133–1138.

Yentekakis I.V., Neophytides S. and Vayenas C.G. (1988), Solid electrolyte aided study of the mechanism of CO oxidation on polycrystalline platinum, *J. Catal.*, **111**, 152-169.

Yentekakis I.V., et al., (2016), Stabilization of catalyst particles against sintering on oxide supports with high oxygen ion lability exemplified by Ir-catalysed decomposition of N_2O, *Appl. Catal. B*, **192**, 357-364.

Yentekakis I.V., et al., (2018), Ir-catalysed nitrous oxide (N_2O) decomposition: Effect of Ir particle size and metal–support interactions, *Catal. Lett.*, **148**, 341-347.

Zhang X., Long E., […] and Chen Y. (2009), CeO_2-ZrO_2-La_2O_3-Al_2O_3 composite oxide and its supported palladium catalyst for the treatment of exhaust of natural gas engined vehicles, *J. Nat. Gas Chem.*, **18**, 139-144.

Zhang, H., Fang S., and Hu Y.H. (2020), Recent advances in single-atom catalysts for CO oxidation, *Catal. Rev.-Sci. Eng.*, doi: 10.1080/01614940.2020.1821443.

Zhu H., et al., (2013), Catalytic methanation of carbon dioxide by active oxygen material $Ce_xZr_{1-x}O_2$ supported Ni-Co bimetallic nanocatalysts, *AlChE J.*, **59**, 2567-2576.

Zou X.-P., Wang L.-N., Li X.-N., Liu Q.-Y., Zhao Y.-X., Ma T.-M. and He S.-G. (2018), Noble-metal-free single-atom catalysts $CuAl_4O_{7-9}^{-}$ for CO oxidation by O_2, *Angew. Chem. Int. Ed.*, **57** 10989-10993.